An Inherently Broadband A- Φ Formulation Solver in Electromagnetics Based on Discrete Exterior Calculus

Boyuan Zhang⁽¹⁾, Dong-Yeop Na⁽²⁾, Dan Jiao⁽¹⁾, and Weng Cho Chew⁽¹⁾

(1) Purdue University, West Lafayette, IN 47907, USA(2) Pohang University of Science and Technology, Pohang, Gyeongbuk 37673, Korea

Abstract—An efficient and inherently broadband numerical solver based on discrete exterior calculus (DEC) for the $A-\Phi$ formulation in electromagnetics is proposed. The $A-\Phi$ formulation with generalized Lorenz gauge is immune to low-frequency breakdown, which makes the proposed solver ideal for broadband and multi-scale analysis. DEC is utilized as the numerical solver to the $A-\Phi$ formulation, where Stokes' theorem and charge conservation are naturally preserved. In addition, DEC can be viewed as a generalized version of finite difference method with unstructured mesh, such as tetrahedral mesh. Thus, complicated multi-scale structures can be discretized easily and efficiently by DEC. Numerical results are presented which indicate the broadband stable nature of the proposed $A-\Phi$ DEC solver over an extremely wide bandwidth (from DC to optics).

I. INTRODUCTION

The E-H formulation in computational electromagnetics (CEM) suffers from low-frequency breakdown due to the null space of the double curl operator. When the frequency is low, or equivalently, when the size of objects is much smaller compared to wavelength, the null space of the double curl operator makes the discretized matrix equation singular. This makes it difficult to use the E-H formulation as a broadband or multi-scale solver in CEM. In contrast, the potential based $A-\Phi$ formulation is free from low-frequency breakdown, thanks to the additional gauge term which cancels the null space of the double curl operator [1], [2]. Thus, the A- Φ formulation is ideal for broadband and multi-scale analysis. In addition, the vector potential **A** and scalar potential Φ are natural bridges connecting classical electromagnetics and quantum electromagnetics. With the rapid development of quantum technology, the incorporation of quantum effects in computational electromagnetics is increasingly important [3].

In this paper, a numerical solver based on discrete exterior calculus (DEC) is proposed to solve the $\mathbf{A}\text{-}\Phi$ formulation with generalized Lorenz gauge [4]. DEC is the discretized version of exterior calculus, which is a mathematical topic from differential geometry. From computational perspective, DEC shares the same spirit with the finite integration technique (FIT) [5]. DEC can be viewed as a generalized version of finite difference method (FDM), where vector calculus identities $\nabla \cdot \nabla = 0$, $\nabla \times \nabla = 0$ and Stokes' theorem are naturally preserved. The preservation of these identities helps to remove spurious charge and maintain structural integrity of Maxwell's equations in the numerical solver. Unstructured mesh, such as triangular mesh in 2D and tetrahedral mesh in 3D, can be

utilized in DEC, which makes capturing complicated multiscale structures easy and efficient.

This paper is organized as follows: In Section II, introduction to the \mathbf{A} - Φ formulation is provided. In Section III, implementation details of the DEC \mathbf{A} - Φ solver are presented. In Section IV, numerical examples are provided to validate the proposed solver and demostrate its broadband stability. In Section V, conclusion of this paper is drawn. In this paper, the time convention $e^{-i\omega t}$ is adopted.

II. \mathbf{A} - Φ FORMULATION

The A- Φ formulation with generalized Lorenz gauge in frequency domain is [4], [6]:

$$\nabla \times \frac{1}{\mu} \nabla \times \mathbf{A} - \omega^2 \tilde{\epsilon} \mathbf{A} - \tilde{\epsilon} \nabla [\chi^{-1} \nabla \cdot (\tilde{\epsilon} \mathbf{A})] = \mathbf{J}, \qquad (1)$$

$$\nabla \cdot (\tilde{\epsilon} \nabla \Phi) + \omega^2 \chi \Phi = -\varrho, \quad (2)$$

where **A** and Φ are the vector potential and scalar potential of the electromagnetic field, respectively; $\tilde{\epsilon} = \epsilon + \frac{i\sigma}{\omega}$ is the complex permittivity; ϵ , μ and σ are the permittivity, permeability and conductivity, respectively; ω is the angular frequency; **J** is the impressed current density and ϱ is the impressed charge density; $\chi = \alpha \mu \tilde{\epsilon}^2$, where α is an arbitrary constant. The following generalized Lorenz gauge from [4] is used in deriving the above equations:

$$\nabla \cdot (\tilde{\epsilon} \mathbf{A}) = i\omega \chi \Phi. \tag{3}$$

Note that in (1), the third term on the left is introduced by the generalized Lorenz gauge, which cancels the null space of the double curl operator [2]. This is the fundamental reason for the inherent broadband stability of the \mathbf{A} - Φ formulation.

In non-static cases ($\omega \neq 0$), (2) can be derived from (1) by taking divergence on both sides of (1), and using the generalized Lorenz gauge (3) along with the charge continuity equation:

$$\nabla \cdot \mathbf{J} = i\omega \rho. \tag{4}$$

Thus, when $\omega \neq 0$, Eqs. (1) and (2) are not independent from each other. Once the **A** equation (1) is solved, one can either solve (2) in tandem with (1) to obtain the Φ result, or simply using (3) to get Φ by

$$\Phi = \frac{\nabla \cdot (\tilde{\epsilon} \mathbf{A})}{i\omega \chi}.$$
 (5)

III. DISCRETE EXTERIOR CALCULUS **A**-Φ SOLVER

A. \mathbf{A} - Φ Equations in DEC

As introduced in Section I, DEC is the discretized version of exterior calculus, and can be viewed as a generalized version of finite difference method (FDM). In DEC, physical quantities are represented by primal/dual cochains, which are the discrete counterparts of primal/dual forms in exterior calculus [6]–[8]. Suppose a simplicial mesh, such as a tetrahedral mesh in 3D cases, is generated in the computational domain, which is referred to as the primal mesh. By using the primal mesh, a dual mesh can be automatically constructed. For example, the barycenters of the primal tetrahedrons and triangles can be used as the dual nodes in the dual mesh. By connecting the dual nodes, dual edges, surfaces and volumes can be further defined. Thus, the dual mesh can be thought as complementary to the primal mesh [6], [7].

In DEC, Φ and $\bf A$ are represented by primal 0-cochians and primal 1-cochains, respectively. The unknown vectors associated with Φ and $\bf A$ are

$$\mathbf{\Phi} = [\Phi_1, \Phi_2, \cdots, \Phi_{N_0}]^T, \tag{6}$$

$$\mathbf{A} = [A_1, A_2, \cdots, A_{N_1}]^T, \tag{7}$$

where N_0 and N_1 are the total number of primal nodes and primal edges in the mesh, respectively; Φ_i is the scalar potential on the *i*-th primal node p_i ; A_i is the integration of **A** along the *i*-th primal edge l_i , namely,

$$A_i = \int_L \mathbf{A} \cdot d\mathbf{l}. \tag{8}$$

Note that Φ_i is the integration of Φ on 0-dimensional objects (nodes) and A_i is the integration of \mathbf{A} on 1-dimensional objects (edges). This explains why Φ_i and A_i are called primal 0-cochain and primal 1-cochian, respectively.

 ${f J}$ and ${\it \varrho}$ are represented by dual 2-cochains and dual 3-cochains in DEC, respectively. The unknown vectors associated with ${f J}$ and ${\it \varrho}$ are

$$J = [J_1, J_2, \cdots, J_{N_1}]^T,$$
 (9)

$$\boldsymbol{\varrho} = [\varrho_1, \varrho_2, \cdots, \varrho_{N_0}]^T, \tag{10}$$

where N_1 is the total number of dual surfaces, which is equal to the total number of primal edges; N_0 is the total number of dual volumes, which is equal to the total number of primal nodes. This is due to the complementary nature between the primal mesh and dual mesh. The definitions of dual 2-cochain J_i and dual 3-cochian ϱ_i are

$$J_i = \int_{S_i^{\text{dual}}} \mathbf{J} \cdot d\mathbf{S},\tag{11}$$

$$\varrho_i = \int_{V_c^{\text{dual}}} \varrho \cdot dV, \tag{12}$$

where S_i^{dual} is the *i*-th dual surface (which is associated with the *i*-th primal edge l_i), and V_i^{dual} is the *i*-th dual volume (which is associated with the *i*-th primal node p_i).

The discrete matrix equations of the $A-\Phi$ formulation (1) and (2) using DEC are

$$\left(\overline{\mathbf{d}}^{(1)}\right)^{T} \star_{\mu^{-1}}^{(2)} \overline{\mathbf{d}}^{(1)} \boldsymbol{A} - \omega^{2} \star_{\epsilon}^{(1)} \boldsymbol{A} + \star_{\epsilon}^{(1)} \overline{\mathbf{d}}^{(0)} \star_{\chi^{-1}}^{(3)} \left(\overline{\mathbf{d}}^{(0)}\right)^{T} \star_{\epsilon}^{(1)} \boldsymbol{A} = \boldsymbol{J}, \quad (13)$$

$$-\left(\overline{\mathbf{d}}^{(0)}\right)^{T} \star_{\epsilon}^{(1)} \overline{\mathbf{d}}^{(0)} \mathbf{\Phi} + \omega^{2} \star_{\chi}^{(0)} \mathbf{\Phi} = -\boldsymbol{\varrho}. \tag{14}$$

where $\overline{\mathbf{d}}^{(i)}$, i=0,1 are called incidence matrices; $\star_{\chi}^{(0)}$, $\star_{\epsilon}^{(1)}$ and $\star_{\mu^{-1}}^{(2)}$ are the Hodge star operators, which correspond to χ , $\tilde{\epsilon}$ and μ^{-1} in (1) and (2).

The dimensions of the incidence matrices $\overline{\mathbf{d}}^{(0)}$ and $\overline{\mathbf{d}}^{(1)}$ are $N_1 \times N_0$ and $N_2 \times N_1$, respectively, where N_2 is the total number of primal surfaces; the superscript (i) indicates $\overline{\mathbf{d}}^{(i)}$ operates on primal i-cochains, and returns primal (i+1)-cochains. The (i,j) elements of $\overline{\mathbf{d}}^{(0)}$ and $\overline{\mathbf{d}}^{(1)}$ are

$$\left[\overline{\mathbf{d}}^{(0)}\right]_{i,j} = d_{i,j}^{(0)} = \begin{cases} \pm 1, & \text{if } p_j \text{ is a vertex of } l_i \\ 0, & \text{otherwise} \end{cases} , \quad (15)$$

$$\left[\overline{\mathbf{d}}^{(1)}\right]_{i,j} = d_{i,j}^{(1)} = \begin{cases} \pm 1, & \text{if } l_j \text{ is an edge of } S_i \\ 0, & \text{otherwise} \end{cases} , \quad (16)$$

where p_i , l_i and S_i denote the i-th primal node, edge and surface, respectively. The sign of the ± 1 entries in (15)-(16) is determined by orientation. In DEC, edges, surfaces and volumes are with positive orientations [7]. If a node p_j is the start/end point of edge l_i , then $d_{i,j}^{(0)} = 1/-1$; if edge l_j and surface S_i have the consistent/opposite orientations (see [6], [7]), $d_{i,j}^{(1)} = 1/-1$. $\overline{\mathbf{d}}^{(0)}$ and $\overline{\mathbf{d}}^{(1)}$ correspond to discrete gradient and curl operations in DEC [6], [7].

There are multiple ways to construct the Hodge star operators $\star_{\chi}^{(0)}, \star_{\epsilon}^{(1)}$ and $\star_{\mu^{-1}}^{(2)}$ [7]–[9]. In this paper, the following Galerkin Hodge star operators are used [6], [10]:

$$\left[\star_{\chi}^{(0)}\right]_{i,j} = \left\langle W_i^0, \chi \cdot W_j^0 \right\rangle,\tag{17}$$

$$\left[\star_{\epsilon}^{(1)}\right]_{i,j} = \left\langle \mathbf{W}_{i}^{1}, \tilde{\epsilon} \cdot \mathbf{W}_{j}^{1} \right\rangle, \tag{18}$$

$$\left[\star_{\mu^{-1}}^{(2)}\right]_{i,j} = \left\langle \mathbf{W}_i^2, \mu^{-1} \cdot \mathbf{W}_j^2 \right\rangle, \tag{19}$$

where W_i^0 is the Whitney 0-form associated with primal node p_i ; \mathbf{W}_i^1 is the Whitney 1-form associated with primal edge l_i ; \mathbf{W}_i^2 is the Whitney 2-form associated with primal surface S_i . χ , $\tilde{\epsilon}$ and μ are piecewise constant parameters within each tetrahedron in the primal mesh; angle brackets denote inner product. Introductions to the Whitney forms can be found in [6] and [11].

Note that the Galerkin Hodge star operators in (17)-(19) are non-diagonal, highly sparse matrices. In (13), $\star_{\chi^{-1}}^{(3)}$ is the inverse of $\star_{\chi}^{(0)}$, which is dense in general. To maintain the sparsity of (13), the sparse approximate inverse (SPAI) technique [12], [13] can be used to find the sparse approximate

of $\star_{\chi^{-1}}^{(3)}$. Alternatively, $\star_{\chi}^{(0)}$ can be constructed as follows based on its geometric interpretation:

$$\left[\star_{\chi}^{(0)}\right]_{i,j} = \begin{cases} \chi V_i^{\text{dual}}, & \text{if } i = j\\ 0, & \text{otherwise} \end{cases} , \tag{20}$$

where V_i^{dual} is the volume of the *i*-th dual mesh. $\star_{\chi}^{(0)}$ in (20) is a diagonal matrix, whose inverse is also diagonal. In this manner, both (13) and (14) are sparse matrix equations, which can be solved by using direct or iterative solvers.

B. Boundary Conditions

The boundary of the computational domain truncates the dual mesh, and proper boundary condition must be implemented in the DEC A- Φ solver. Due to the page limit, one can refer to [6], [8] for further details on implementing different boundary conditions.

IV. NUMERICAL EXAMPLES

In this section, numerical examples are provided to validate the DEC A- Φ solver for both quasi-static physics and wave physics. The broadband stability of the proposed solver is demonstrated. Note that the capability of the DEC A- Φ solver in solving multi-scale problems is implied by its broadband stability, since one can solve for quasi-static physics and wave physics with equally good accuracy the multi-scale simulations.

A. Rectangular Wire Loop

The dimension of the copper rectangular loop along with the tetrahedral mesh are shown in Fig. 1. The size of the square cross section of the wire loop is 10 nm by 10 nm. The copper wire loop is excited by the impressed current J in the 2 nm thick excitation gap. Extracted resistance and inductance of the wire loop with PEC boundary condition are listed in Table I. Also listed are the reference results by using Ohm's law and approximate formula from [14]. It should be noticed that the approximate formulae are for engineering purposes, which could only provide a ballpark number to verify that the DEC A- Φ results are within a reasonable range. As can be seen, the results obtained by using the DEC A- Φ solver are stable over a wide frequency spectrum.

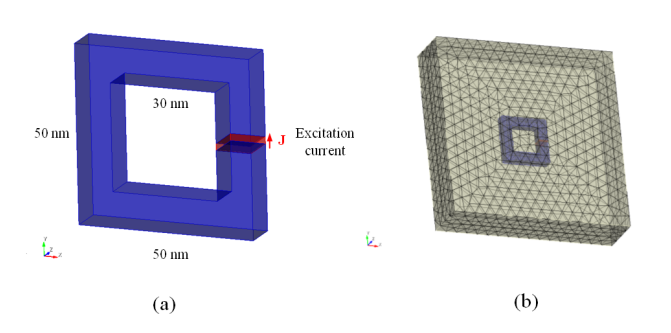


Fig. 1. (a) Dimension and (b) tetrahedral mesh of the rectangular wire loop example.

TABLE I CALCULATED INPUT IMPEDANCE Z, RESISTANCE R, AND INDUCTANCE L OF THE WIRE LOOP

Frequency (Hz)	$Z(\Omega)$	$R(\Omega)$	L(H)
1k	$23.88 - i2.51 \times 10^{-10}$	23.88	4.00×10^{-14}
1M	$23.88 - i2.53 \times 10^{-7}$	23.88	4.03×10^{-14}
100M	$23.88 - i2.59 \times 10^{-5}$	23.88	4.12×10^{-14}
1G	$23.88 - i2.59 \times 10^{-4}$	23.88	4.12×10^{-14}
10G	$23.88 - i2.60 \times 10^{-3}$	23.88	4.13×10^{-14}

The approximate reference resistance is $R=27.84~\Omega$ and inductance $L=3.611\times 10^{-14}~\mathrm{H}.$

B. Rod Antenna

The rod antenna case from [15] is studied in this section, as shown in Fig. 2. The rod antenna is composed of two pieces of copper with the excitation gap between them. The length of each copper segment is 7.238 mm, with square cross section 0.517 mm by 0.517 mm. The thickness of the excitation gap is 0.517 mm, making the total length of the antenna L=14.993 mm. The rod antenna is in a cubic vacuum box with length 40 mm, and the impedance boundary condition (IBC) is applied as the absorbing boundary condition. Figs. 3 and 4 show the real and imaginary parts of the input impedance Z of the antenna from the DEC solver and [15] under different frequencies. Two sets of tetrahedral meshes have been used to obtain the DEC results to demonstrate that convergence has been achieved in terms of mesh size. Overall agreement between the DEC results and the reference result can be observed with some deviations. The deviations can be attributed to two reasons: first, the reference result from [15] is computed by using finite difference time domain (FDTD) method with Gaussian pulse excitations, followed by Fourier transform, while the DEC results are obtained in frequency domain directly. Second, the absorbing boundary condition used in [15] is perfect matched layers (PML), whereas IBC is used in the present DEC simulations. These two differences in the simulations can potentially introduce numerical discrepencies to the results. Nevertheless, the proposed DEC $A-\Phi$ solver can be validated in this rod antenna case with radiating wave physics.

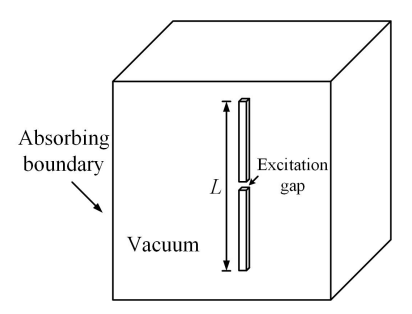


Fig. 2. Illustration of the rod antenna case from [15].

C. Broadband Stability

To further demonstrate the broadband stability of the DEC $A-\Phi$ solver, the size of the rod antenna is reduced to nano-

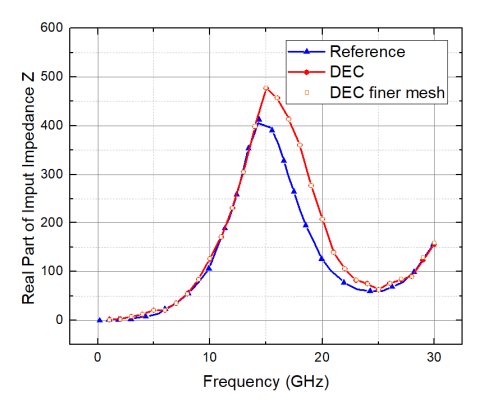


Fig. 3. Real part of the input impedance Z from [15] and DEC.

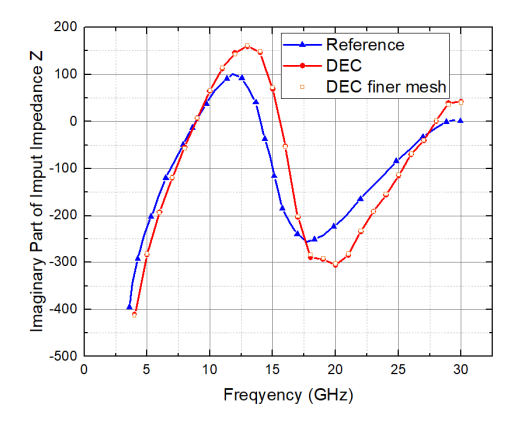


Fig. 4. Imaginary part of the input impedance Z from [15] and DEC.

scale, with total length $L=500\,$ nm. The cross section is 10 nm by 10 nm, and the thickness of the excitation gap is 10 nm. The cubic vacuum box has length 1000 nm with PEC boundary condition. The input impedance Z, resistance (real part of Z) and capacitance of the rod antenna within an extremely wide spectrum, from 10 Hz (DC) to 10 THz (infrared), are extracted by using the proposed solver, as shown in Fig. 5. Clearly, the DEC results are very stable over the entire spectrum. Note that when f=1 THz, it is close to the resonance frequency of the rod antenna; thus the imaginary part of Z starts to oscillate. To the authors' best knowledge, there is no other work that can simulate over such a wide spectrum, and thus no reference results can be presented. This example clearly demonstrates the broadband stability of the DEC solver.

V. CONCLUSION

In this paper, an inherently broadband DEC $A-\Phi$ solver is proposed. Introduction to the $A-\Phi$ formulation as well as the implementation details of the proposed solver are provided. Numerical examples are presented to validate the proposed solver and demonstrate its stability over an extremely broad spectrum (from DC to optics). The proposed solver preserves Stokes' theorem and charge conservation with unstructured mesh schemes. Thus, the DEC $A-\Phi$ solver is ideal for

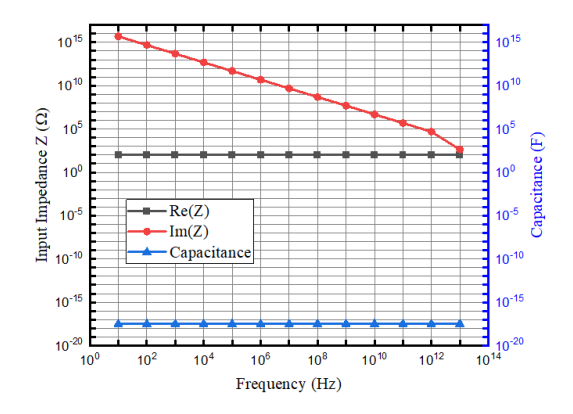


Fig. 5. The extracted input impedance Z, resistance and capacitance of the nano-scale rod antenna from 10 Hz to 10 THz.

broadband and multi-scale analysis with high accuracy and efficiency.

REFERENCES

- Y. Zhao and W. N. Fu, "A new stable full-wave Maxwell solver for all frequencies," *IEEE Transactions on Magnetics*, vol. 53, no. 6, pp. 1–4, 2016.
- [2] Y. Li, Advanced finite element methodology for low-frequency and static electromagnetic modeling, Ph.D. dissertation, The University of Hongkong, 2015.
- [3] W. C. Chew, D.-Y. Na, P. Bermel, T. Roth, C. J. Ryu, and E. Kudeki, "Quantum Maxwell's equations made simple: Employing scalar and vector potential formulation," *IEEE Antennas and Propagation Magazine*, vol. 63, no. 1, pp. 14–26, 2020.
- vol. 63, no. 1, pp. 14–26, 2020.
 [4] W. C. Chew, "Vector potential electromagnetics with generalized gauge for inhomogeneous media: formulation," *Progress In Electromagnetics Research*, vol. 149, pp. 69-84, 2014.
- [5] C. Markus, and T. Weiland. "Discrete electromagnetism with the finite integration technique." *Progress In Electromagnetics Research*, vol. 32, pp. 65-87, 2001.
- [6] B. Y. Zhang, D.-Y. Na, D. Jiao and W. C. Chew, "An A-Φ formulation solver in electromagnetics based on discrete exterior calculus", *IEEE Journal on Multiscale and Multiphysics Computational Techniques*, accepted.
- [7] S. C. Chen and W. C. Chew, "Numerical electromagnetic frequency domain analysis with discrete exterior calculus," *Journal of Computational Physics*, vol. 350, pp. 668–689, 2017.
- [8] J. Räbinä, On a numerical solution of the Maxwell equations by discrete exterior calculus, Ph.D. dissertation, University of Jyväskylä, 2014.
- [9] T. Tarhasaari, L. Kettunen, and A. Bossavit, "Some realizations of a discrete Hodge operator: a reinterpretation of finite element techniques [for EM field analysis]," *IEEE Transactions on Magnetics*, vol. 35, no. 3, pp. 1494–1497, 1999.
- [10] H. Bo and F. L. Teixeira, "Geometric finite element discretization of Maxwell equations in primal and dual spaces," *Physics Letters A*, vol. 349, no. 1-4, pp. 1–14, 2006.
- [11] J. M. Jin, The Finite Element Method in Electromagnetics. John Wiley & Sons, 2015.
- [12] M. J. Grote and T. Huckle, "Parallel preconditioning with sparse approximate inverses," SIAM Journal on Scientific Computing, vol. 18, no. 3, pp. 838–853, 1997.
- [13] J. Kim and F. L. Teixeira, "Parallel and explicit finite-element timedomain method for Maxwell's equations," *IEEE Transactions on Antennas* and Propagation, vol. 59, no. 6, pp. 2350–2356, 2011.
- [14] F. W. Grover, Inductance Calculations: working formulas and tables. Courier Corporation, 2004.
- [15] K. Yoshitomi, "A study on current sources used in finite-difference time-domain antenna analysis," in 2007 IEEE Applied Electromagnetics Conference (AEMC), Kolkata, India, Dec. 2007, pp. 1–4.